ISBN: 978-3-95450-216-5 doi:10.18429/JACoW-eeFACT2018-TUYBA02

BEAM-BEAM EFFECTS AT HIGH ENERGY e+e− COLLIDERS*

D. Shatilov†, Budker Institute of Nuclear Physics, 630090 Novosibirsk, Russia

Abstract

One of the main requirements for future e+e− colliders is high luminosity. If the energy per beam does not exceed 200 GeV, the optimal choice will be a circular collider with "crab waist" collision scheme. Here, to achieve maximum luminosity, the beams should have a very high density at the IP. For this reason, radiation in the field of a counter bunch (BS – beamstrahlung) becomes an appreciable factor affecting the dynamics of particles. In particular, in the simulations for Further Circular Collider (FCC), new phenomena were discovered: 3D flip-flop and coherent X-Z instability. The first is directly related to BS. The second can manifest itself at low energy (where BS is negligible), but at high energies BS substantially changes the picture. In the example of FCC-ee, we will consider the features of beam-beam interaction at high-energy crab waist colliders, and optimization of parameters for high luminosity.

INTRODUCTION

FCC-ee is a double-ring e+e− collider to be built at CERN and operate in the wide energy range from Z-pole (45.6 GeV) to ttbar (up to 185 GeV). At such energies, beam-beam effects can get an extra dimension due to BS [1, 2]. FCC-ee apparently will be the first collider where BS plays a significant role in the beam dynamics. For this to happen, two conditions must be fulfilled: high energy and high charge density in the bunch. For example, the energy in LEP was large enough, but the charge density too small, so the effect was negligible. BS increases the energy spread (and hence the bunch length) and creates long non-Gaussian tails in the energy distribution, which can limit the beam lifetime due to a possible escape of particles beyond the energy acceptance.

The collider has a two-fold symmetry and two Interaction Points (IP) with a horizontal crossing angle and "crab waist" collision scheme [3, 4]. The luminosity per IP for flat beams ($\sigma_y << \sigma_x$) can be written as:

$$L = \frac{\gamma}{2er_e}\cdot\frac{I_{tot}\xi_y}{\beta_y^*}\cdot R_H\,, \qquad (1)$$

where I_{tot} is the total beam current which is determined by the synchrotron radiation power 50 MW. Therefore L can be increased only by making ξ_y larger and β_y^* smaller while keeping R_H reasonably large. We assume that ξ_y can be easily controlled by N_p (number of particles per bunch), that implies adjusting the number of bunches to keep I_{tot} unchanged. The hour-glass factor R_H depends on L_i/β_y^* ratio, where L_i is the length of interaction area which in turn depends on σ_z and Piwinski angle ϕ:

$$\phi = \frac{\sigma_z}{\sigma_x}tg\left(\frac{\theta}{2}\right), \qquad (2)$$

$$L_i = \frac{\sigma_z}{\sqrt{1+\phi^2}} \Rightarrow \frac{2\sigma_x}{\theta}. \qquad (3)$$

Here θ is the full crossing angle, and expressions after $\Rightarrow$ correspond to $\phi >> 1$ and $\theta << 1$, see Fig. 1.

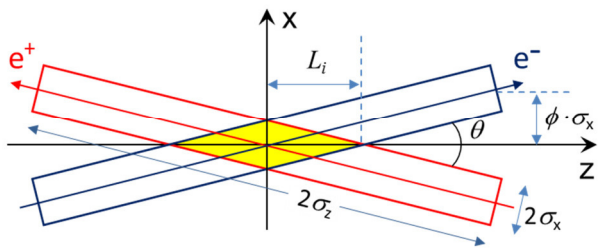

Figure 1: Sketch of collision with large Piwinski angle.

The beam-beam parameters for $\sigma_y << \sigma_x$ and $\theta \neq 0$ become [5]:

$$\xi_x = \frac{N_p r_e}{2\pi\gamma}\cdot\frac{\beta_x^*}{\sigma_x^2(1+\phi^2)} \Rightarrow \frac{N_p r_e}{\pi\gamma}\cdot\frac{2\beta_x^*}{(\sigma_z\theta)^2}$$
$$\xi_y = \frac{N_p r_e}{2\pi\gamma}\cdot\frac{\beta_y^*}{\sigma_x\sigma_y\sqrt{1+\phi^2}} \Rightarrow \frac{N_p r_e}{\pi\gamma}\cdot\frac{1}{\sigma_z\theta}\sqrt{\frac{\beta_y^*}{\varepsilon_y}} \qquad (4)$$

In particular, $\xi_x \propto 1/\varepsilon_x$ (in head-on collision) transforms to $\xi_x \propto \beta_x^*/\sigma_z^2$ when $\phi >> 1$, and ξ_y dependence on σ_x vanishes. Further, because of the symmetry, we consider a model with one IP (that is a half ring of FCC-ee).

HIGH ENERGY

At very high energies (e.g. ttbar production, 175÷185 GeV) the beam lifetime is mainly determined by single BS photons [2], which imposes another limitation on the luminosity. An example is shown in Fig. 2. The black curve corresponds to the Gaussian distribution with σ_δ increased by 30% due to BS. As is seen, within 3-4 sigma the real distribution agrees well with it, but at large amplitudes there are long non-Gaussian tails. Their asymmetry is related to the fact that the damping time is comparable

* Work supported by Russian Science Foundation, N 14-50-00080.
† email: shatilov@inp.nsk.su

ISBN: 978-3-95450-216-5 doi:10.18429/JACoW-eeFACT2018-TUYBA02

to the period of synchrotron oscillations. Therefore, the optimized momentum acceptance also should be asymmetrical, as proposed and implemented in [6, 7].

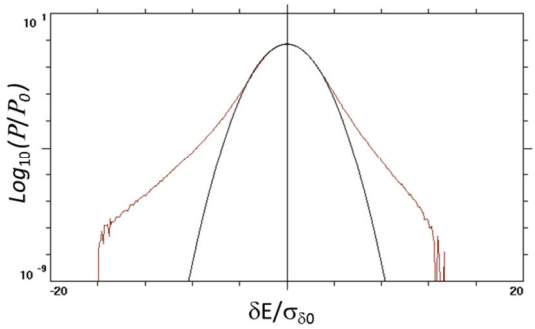

Figure 2: Energy distribution at 182.5 GeV in the logarithmic scale, black line: Gauss with $\sigma_\delta = 1.3\ \sigma_{\delta 0}$.

A rough estimate for the beamstrahlung lifetime can be found in [8]:

$$\tau_{BS} \propto \exp\left(\frac{2\alpha\eta\rho}{3r_e\gamma^2}\right)\cdot\frac{\rho\sqrt{\eta\rho}}{L_i\gamma^2}, \qquad (5)$$

where α is a fine structure constant, η is the energy acceptance (which should be maximized), and ρ is the bending radius of particle's trajectory in the field of oncoming bunch. Evidently, ρ is inversely proportional to the absolute value of transverse electro-magnetic force acting on the particle. Its dependence on the transverse coordinates for flat beams is shown in Fig. 3.

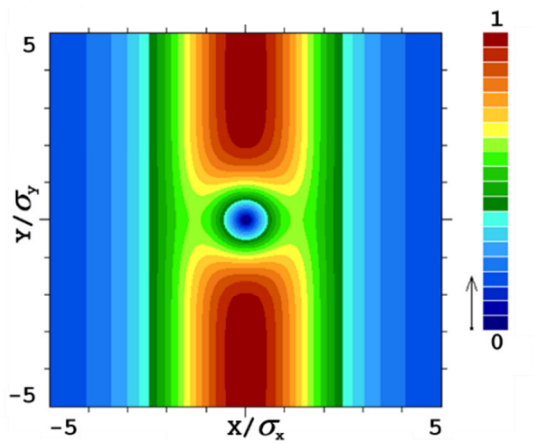

Figure 3: Absolute value of the transverse force for flat beams, in relative units.

The minimum values of ρ correspond to the particles with $|x| < \sigma_x/2$ and $|y| > 2\sigma_y$. However, during collision particles traverse the opposite bunch horizontally because of the crossing angle. This means that the maximum force acting on a particle at the IP depends mainly on the vertical coordinate, and ρ is inversely proportional to the surface charge density in the horizontal plane:

$$\frac{1}{\rho} \propto \frac{N_p}{\gamma\sigma_x\sigma_z} \propto \frac{\xi_y}{L_i}\sqrt{\frac{\varepsilon_y}{\beta_y^*}} \propto L\sqrt{\frac{\varepsilon_y}{\beta_y^*}}. \qquad (6)$$

These relations are valid for both head-on and crossing angle collisions; the last transformation is based on (1) and assumption that $L_i \approx \beta_y^*$.

Our goal is to increase L while keeping the lifetime (and therefore ρ) large enough. It follows that ε_y (i.e. both the betatron coupling and ε_x) should be minimized, and β_y^* should be *increased*. For example, increase in β_y^* (together with L_i) by a factor of k may result in the luminosity gain by $k^{1/2}$ with ρ unchanged. In fact, as is seen from (5), τ_{BS} is inversely proportional to L_i provided that $\rho = const$. Therefore, to keep $\tau_{BS} = const$ when L_i is increased, we need to slightly increase ρ. However, τ_{BS} dependence on L_i is much weaker than the dependence on ρ (because the argument of *exp* is >> 1), so the gain in luminosity will be *almost* $k^{1/2}$. All these manipulations mean an increase in σ_x and N_p, but other than that, ξ_y will also rise by $k^{3/2}$. Consequently, we may perform such optimization only as long as ξ_y remains below the beam-beam limit.

This can be formulated in a different way. If there are multiple limiting factors, the maximum performance is achieved when all limits are reached simultaneously. In our case it means that β_y^* (together with L_i) should be adjusted in such a way that both τ_{BS} and ξ_y achieve their limits. This implies that, if the balance shifts towards "limit by the BS lifetime" (e.g. decrease in η or increase in γ, ε_y), the luminosity optimization will require some increase in L_i (together with β_y^*).

Note that in collision with large Piwinski angle, an increase in L_i means an increase in σ_x rather than σ_z. Since ε_y should be small, L_i is controlled by β_x^* which is made quite large, unlike lower energies, where the choice of β_x^* is determined by other factors.

3D FLIP-FLOP

When energy decreases, the lifetime limitation due to BS weakens. This is easy to understand from the following considerations. Assuming that the lattice is not changed, emittances drop quadratically and σ_x, L_i – linearly with energy. If we keep ξ_y and β_y^* unchanged then, as follows from (5) and (6), ρ remains constant and τ_{BS} grows significantly because its dependence on γ is very strong. Hence at lower energies we may allow some reduction in η, and for higher luminosity we need to decrease β_y^* and ρ. On the other hand, since the bending radius in the arc dipoles remains unchanged, the relative contribution of BS to the energy spread grows and the bunch lengthening becomes larger.

For example, when the parameters of FCC-ee are optimized for high luminosity, σ_z increases due to BS almost 3.5 times at 45.6 GeV and only 1.3 times at 182.5 GeV. Why then we do not see this effect in low energy colliders? Because they have much higher magnetic field in the

ISBN: 978-3-95450-216-5 doi:10.18429/JACoW-eeFACT2018-TUYBA02

dipoles or, which is the same, much smaller bending radius in the arcs.

As seen from (4), the bunch lengthening leads to a decrease in ξ_y and L. Therefore, to achieve high luminosity, it is necessary to increase N_p. That, in turn, strengthens BS and causes additional lengthening. As a result, the equilibrium σ_z with account of BS can increase several times, and this is fraught with the appearance of instability. The threshold depends on asymmetry in population of colliding bunches, but even in a symmetrical case the instability arises (with higher N_p).

Briefly, the problem is that the weakening of BS for one bunch leads to its shortening, as a result ξ_x and ξ_y for the opposite bunch grow and all three of its sizes are increasing; this even more weakens the BS for the first bunch. In this way we obtain a positive feedback in the following chain:

1) Asymmetry in the bunch currents leads to asymmetry in the bunch lengths (due to BS).
2) In collisions with $\phi >> 1$, asymmetry in σ_z enhances synchrotron modulation of the horizontal kick for a longer bunch, thus amplifying synchro-betatron resonances. Besides, ξ_x^w grows quadratically and ξ_y^w – linearly with decrease of σ_z^s, so the footprint expands and can cross more resonances. All this leads to increase in both emittances of the weak bunch.
3) An increase in ε_x^w has two consequences: a) weakening of BS for a strong bunch, which makes it shorter, and b) growth of ε_y^w due to the betatron coupling, which leads to asymmetry in the vertical beam sizes.
4) As seen in Fig. 3, the greatest BS is experienced by the particles with the vertical coordinates $|y^w| > 2\sigma_y^s$. When $\sigma_y^w > \sigma_y^s$, the number of particles in the weak bunch experiencing strong BS increases while the number of such particles in the strong bunch decreases. Thus, asymmetry in the vertical beam sizes leads to further increase in σ_z asymmetry.
5) Now we go back to point 2, and the loop is closed. In the beginning, all three beam sizes grow slowly until the footprint touches strong resonance, then the "weak" bunch blows up.

An example is shown in Fig. 4. The top row corresponds to a stable situation, though some acceptable bloating of the weak bunch is seen. In the bottom row asymmetry is the same, but N_p increased by 5%. As a result, the strong bunch shrank to unperturbed sizes, while the weak one became swollen in all three dimensions.

Another example can be found in [9], where the strength of "crab" sextupoles was not optimal. In this case ξ_y^w exceeds the limit, which leads to bloating of σ_y^w. Thus we come to asymmetry in σ_y, and instability begins to develop in the longitudinal and vertical dimensions. At the same time, ξ_x^w grows rapidly with decreasing σ_z^s, and when the footprint overlaps horizontal synchro-betatron resonance, σ_x^w also increases, making the whole process even faster. In the end, we again get 3D flip-flop.

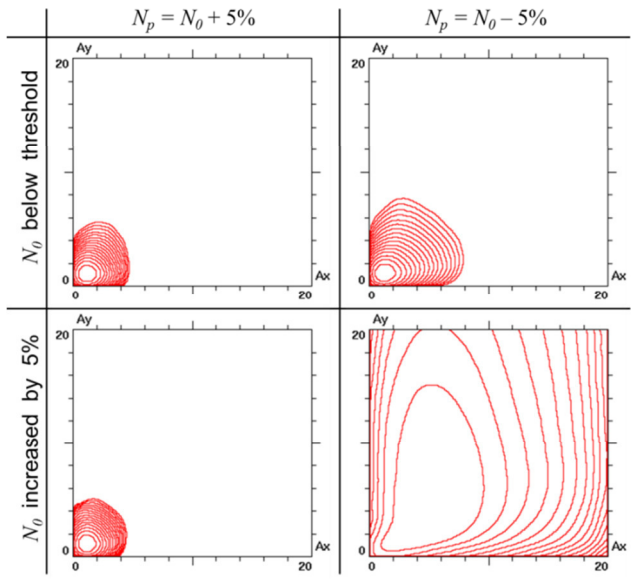

Figure 4: Example of 3D flip-flop. Equilibrium density contour plots ($\sqrt{e}$ between successive lines) in the space of normalized betatron amplitudes are shown for stable (top) and unstable (bottom) cases.

In the best case, when crab sextupoles are optimal and ξ_y below the limit, the 3D flip-flop is usually initiated by the horizontal synchro-betatron resonances – satellites of half integer. This is its similarity with another instability, which will be discussed below.

COHERENT X-Z INSTABILITY

This instability [10, 11] develops in the horizontal plane and is manifested by wriggle of the bunch shape. If we imagine that the bunch is sliced longitudinally in many pieces, the amplitudes of X-displacement of slices depend on their Z-coordinates and vary on every turn. An example is presented in Fig. 5, where coordinates of centers of slices are shown at some turns. Red line corresponds to unperturbed state, green – to the stage of development of instability (oblique part of the curve in Fig. 6), and blue – to the final stage with ε_x blown up.

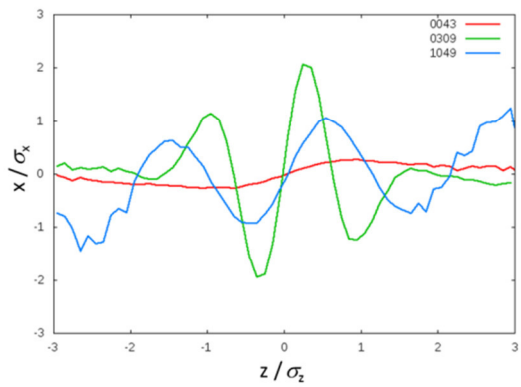

Figure 5: Coherent X-Z instability, the bunch shape in the horizontal plane at different (43, 309 and 1049) turns.

ISBN: 978-3-95450-216-5 doi:10.18429/JACoW-eeFACT2018-TUYBA02

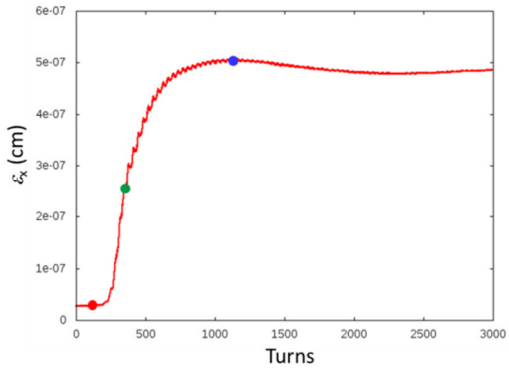

Figure 6: Evolution of the horizontal emittance. The colour dots correspond to the turns shown in Fig. 5.

In collision schemes with $\phi >> 1$, an increase in ε_x itself does not have a noticeable impact on luminosity. However, this leads to a proportional increase in ε_y due to the betatron coupling, so eventually the luminosity will drop several times. The instability does not cause dipole oscillations and therefore cannot be suppressed by feedback. We need to look for conditions under which it does not arise.

The most effective is to reduce β_x^*, which means a decrease in ξ_x. However, in FCC-ee at 45.6 GeV, β_x^* can only be reduced to 15 cm [7, 12], and this is not enough to suppress the instability. The next step is to reduce ξ_x with the given β_x^*. In fact ξ_x is important not itself, but in comparison with the synchrotron tune ν_s. As we shall see later, the greatest danger arises from the synchro-betatron resonances $2\nu_x - 2m\cdot\nu_s = 1$, the distance between them is just ν_s. Our task is to make ξ_x noticeably smaller than ν_s, then we can put the working point and the whole footprint between resonances. Herewith, by decreasing ξ_x we should preserve the luminosity, i.e. ξ_y. In assumption that $\beta_{x,y}^*$ and ε_y were already minimized and therefore are not free parameters, from (4) it follows that the only way to reduce the ξ_x/ξ_y ratio is to increase the bunch length (we assume that N_p also should grow proportionally, to keep ξ_y unchanged).

This is best done by increasing the momentum compaction factor α_p. An advantage is that ν_s grows together (and by the same factor) with σ_z. In addition, larger α_p increases the threshold of microwave instability to an acceptable level. The main drawback of this approach is that emittances also grow in the power of 3/2 with respect to α_p, and yet we were forced to double α_p at 45.6 GeV [7, 12].

Further optimization requires a proper choice of the working point. For this we performed a scan of betatron tunes in a simplified model: linear lattice without explicit betatron coupling. The beam-beam effects were implemented in a weak-strong approximation; therefore coherent instabilities are not manifested here. The simulation results are presented in Fig. 7. Since $\xi_x << \xi_y$, the footprint looks like a narrow vertical strip, bottom edge resting on the working point.

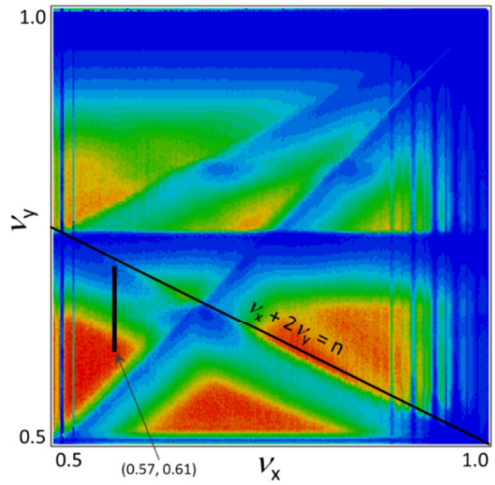

Figure 7: Luminosity for FCC-ee at 45.6 GeV, depending on the betatron tunes. The colour scale from zero (blue) to $2.3\cdot10^{36}$ cm^{-2}c^{-1} (red). The black narrow rectangle shows the footprint at (0.57, 0.61).

The good region is reduced to a red triangular area bounded by the main coupling resonance $\nu_x = \nu_y$, sextupole resonance $\nu_x + 2\nu_y = n$, and half-integer resonance $2\nu_x = 1$ with its synchrotron satellites. All other higher-order coupling resonances are suppressed by the crab waist, and therefore are not visible. As seen from the plot, the range of permissible ν_x for large ξ_y is bounded on the right by 0.57 – 0.58.

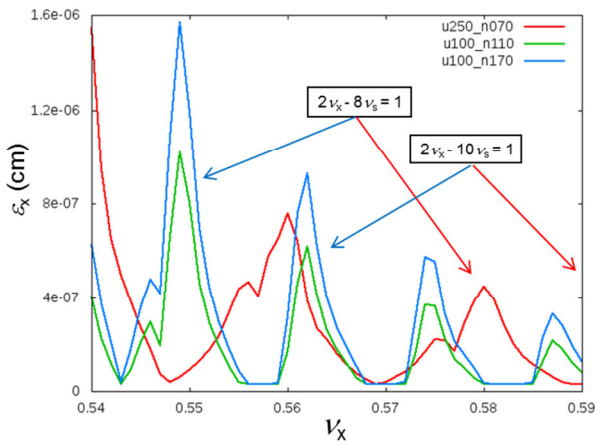

Figure 8: Growth of ε_x due to coherent X-Z instability, depending on ν_x, for FCC-ee at 45.6 GrV. Red line corresponds to U_{RF} = 250 MV, $N_p = 7\cdot10^{10}$, green and blue lines – U_{RF} = 100 MV, $N_p = 1.1\cdot10^{11}$ and $1.7\cdot10^{11}$.

Then we performed a numerical scan of ν_x in quasi-strong-strong model, in which coherent instabilities and flip-flop can be observed. The results are presented in Fig. 8, and synchro-betatron resonances are clearly seen. As the order of resonances increases, their strength weakens. Zones free from instability can be detected starting from the region between $2\nu_x - 8\nu_s = 1$ and $2\nu_x - 10\nu_s = 1$,

ISBN: 978-3-95450-216-5 doi:10.18429/JACoW-eeFACT2018-TUYBA02

so the "good" ν_x are determined by the synchrotron tune. As seen, the first window for U_{RF} = 250 MV is located around 0.59 – too much for large ξ_y. And here we are helped by the reduction of U_{RF}, thereby decreasing ν_s (while ξ_x/ν_s not changed) and increasing the order of resonances located in the region of interest ($\nu_x < 0.58$).

Here it is appropriate to recall the semi-analytical scaling law obtained from other considerations for the threshold bunch intensity [12]:

$$N_{th} \propto \frac{\alpha_p \sigma_\delta \sigma_z}{\beta_x^*}, \qquad (7)$$

where σ_δ is the energy spread. In respect that $\alpha_p\sigma_\delta \propto \nu_s\sigma_z$ and $\xi_x \propto N_p\beta_x^*/\sigma_z^2$, this is nothing else than a condition on the ratio ξ_x/ν_s. We obtained a similar relation from the simple requirement to "squeeze" the footprint in between synchro-betatron resonances. It should be noted that the proposed solution also solves the problem with 3D flip-flop, since it helps to avoid resonances which are crucial for both instabilities.

Consider now the influence of BS on these processes. In our range of parameters, where σ_z is defined mainly by BS, it scales as $\sigma_z^2 \propto N_p$. The rationale for this dependence is not so obvious, but in the simulation it was confirmed with good accuracy. As a result, ξ_x does not depend on N_p. This is clearly seen in Fig. 8 comparing the green and blue lines, which differ only in the bunch population. Thus, if we stay in a "good" area, N_p can be increased until it is limited by other factors – energy acceptance or ξ_y. The reverse side of this coin is that getting rid of instability (e.g. if ν_x is not optimal) simply by reducing N_p will be quite difficult. To do this, it is necessary to descend to the region where the dependence $\sigma_z^2 \propto N_p$ is violated, which means a significant decrease in the luminosity.

BOOTSTRAPPING

Another problem is how to bring bunches into collision, since "before collision" they are too short. Consequently, $\xi_{x,y}$ will be far above the limits, and the beams will be blown up and killed on the transverse aperture before they are stabilized by BS. To avoid this, we must gradually increase the bunch population during collision, so we come to *bootstrapping*.

An example is presented in Fig. 9. We start with approximately one quarter of the final bunch population, and then alternately add small portions to both beams. In fact, the injection cycle will last about 2 minutes, but in simulations it was reduced to ~2 damping times to avoid unnecessary time-consuming calculations.

As is seen, the bunch after injection (added portion) becomes "strong" and its length reduces because the opposite bunch elongates due to the increased beamstrahlung, while the asymmetry remains moderate all the time.

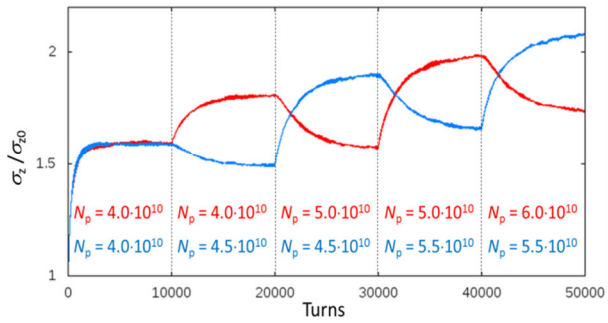

Figure 9: Simulated bootstrapping for Z-pole operation in FCC-ee: length of colliding bunches vs. time. The first few steps towards the nominal $N_p = 1.7\cdot10^{11}$ are shown.

The benefit of this procedure is especially great at low energies, where it can double the luminosity. But also at high energies the luminosity can be raised using this method and avoiding large asymmetry in the population of colliding bunches.

PARAMETER OPTIMIZATION SUMMARY

With increasing energy, Piwinski angle decreases and damping becomes stronger, so the coherent instabilities weaken. In addition, when considering the optimization of parameters, it is necessary to take into account that a resonant depolarization (which may be required for energy calibration) imposes a restriction on the synchrotron tune [13].

Here we briefly describe the selection of parameters associated with the beam-beam interaction at four FCC-ee operating points (see also in [7, 14]). The current table can be found in [15].

Z-pole (45.6 GeV)

The biggest problems at this energy are associated with the 3D flip-flop and coherent X-Z instability. To combat them, the following steps were taken: increase α_p, decrease β_x^* and U_{RF}, choice of ν_x between synchro-betatron resonances in the range from 0.56 to 0.58.

$W^\pm$ Pair Production Threshold (80 GeV)

Here we may allow smaller α_p to decrease emittances, while the instabilities are mitigated by low β_x^* and U_{RF}. However, in this case ν_s will be too small. In order to make a resonant depolarization possible, we were forced to use the lattice with large α_p (same as at Z-peak) and the maximum possible U_{RF}, which is determined by the RF staging scenario. A small β_x^* and proper choice of betatron tunes are sufficient to avoid instabilities.

HZ Production (120 GeV)

At this and the next energy points we do not care about polarization, therefore α_p should be small to minimize emittances, while U_{RF} is determined by the energy loss per turn – there is not much freedom for optimization.

ISBN: 978-3-95450-216-5 doi:10.18429/JACoW-eeFACT2018-TUYBA02

The coherent instabilities at 120 GeV are much weaker but still exist; the remedy is the same as above: a small β_x^* and a neat choice of the working point.

ttbar Threshold (175 – 182.5 GeV)

The coherent instabilities are suppressed by very strong damping, but another problem becomes dominant: the lifetime limitation by single high-energy BS photons. Therefore, in contrast to other energies, optimization requires an increase in β_x^*.

It is worth recalling that the condition $\beta_y^* \approx L_i$ should be met at all points, which actually means an increase in β_y^* with energy.

ACKNOWLEDGEMENTS

The author would like to thank K. Oide and K. Ohmi for many useful discussions.

REFERENCES

[1] J. Augustin *et al*., "Limitations on performance of e+e− storage rings and linear colliding beam systems at high energy", *eConf* C781015, 009, 1978.

[2] V. Telnov, "Restriction on the energy and luminosity of e+e− storage rings due to beamstrahlung", *Phys. Rev. Lett.* vol. 110, p. 114801, Mar. 2013.

[3] P. Raimondi, D. Shatilov, and M. Zobov, "Beam-beam issues for colliding schemes with large Piwinski angle and crabbed waist", LNF-07-003-IR, Jan. 2007, e-Print: physics/0702033.

[4] M. Zobov *et al*., "Test of crab waist collisions at DAFNE Phi factory", *Phys. Rev. Lett.* vol. 104, p. 174801, Apr. 2010.

[5] P. Raimondi and M. Zobov, "Tune shift in beam-beam collisions with a crossing angle", DAFNE Tech. Note G-58, Apr. 2003.

[6] K. Oide, "Optics for Compton scattering", 64th FCC-ee Optics Design meeting, CERN, Nov. 2017, https://indico.cern.ch/event/683544/.

[7] K. Oide, "FCC-ee optics design", ICFA Beam Dyn. Newslett. 72, p. 19, Dec. 2017.

[8] A. Bogomyagkov, E. Levichev, and D. Shatilov, "Beam-beam effects investigation and parameters optimization for a circular e+e− collider at very high energies", *Phys. Rev. ST Accel. Beams,* vol. 17, p. 041004, Apr. 2014.

[9] K. Ohmi, "CEPC and FCCee parameters from the viewpoint of the beam-beam and electron cloud effects", IAS High Energy Physics Conf., Hong Kong, Jan. 2018.

[10] K. Ohmi, "Study of coherent head-tail instablility due to beam-beam interaction in cirular colliders based on crab waist scheme", in *Proc. eeFACT2016*, Daresbury, UK, Oct. 2016, paper TUT1BH2, pp. 61-65.

[11] K. Ohmi, *et al*., "Coherent beam-Beam instability in collisions with a large crossing angle", *Phys. Rev. Lett*. vol. 119, p. 134801, Sep. 2017.

[12] K. Oide *et al*., "Progress in the design of beam optics for FCC-ee collider ring", in *Proc. IPAC2017*, Copenhagen, Denmark, May 2017, paper TUOCB1, pp. 1281-1284.

[13] I. Koop, "Polarization studies for FCC-ee and CEPC", presented at FCC Week 2018, Amsterdam, Netherlands, Apr. 2008, https://indico.cern.ch/event/656491/contributions/2938716/.

[14] D. Shatilov, "FCC-ee parameter optimization", ICFA Beam Dyn. Newslett. 72, p. 30, Dec. 2017.

[15] D. Shatilov, "IP beam parameter optimization for FCC-ee", presented at FCC Week 2018, Amsterdam, Netherlands, Apr. 2008, https://indico.cern.ch/event/656491/contributions/2939184/.